Carbohydrate Polymers 97 (2013) 695–702

Contents lists available at SciVerse ScienceDirect

Carbohydrate Polymers

journal homepage: www.elsevier.com/locate/carbpol

Extraction of cellulose nanofibrils from dry softwood pulp using high shear homogenization

Jiangqi Zhao[a], Wei Zhang[a,*], Xiaodan Zhang[b], Xinxing Zhang[a], Canhui Lu[a], Yulin Deng[b]

[a] State Key Laboratory of Polymer Materials Engineering, Polymer Research Institute at Sichuan University, Chengdu 610065, China
[b] School of Chemical and Biomolecular Engineering and IPST at GT, Georgia Institute of Technology, Atlanta 30332-0620, Georgia

ARTICLE INFO

Article history:
Received 15 February 2013
Received in revised form 4 April 2013
Accepted 20 May 2013
Available online 25 May 2013

Keywords:
Cellulose nanofibrils
Crystallinity
High shear homogenization
Refining
Thermal properties

ABSTRACT

The objective of this study was to extract cellulose nanofibrils (CNFs) from dry softwood pulp through a simple and environmentally friendly physical method of refining pretreatment coupled with high shear homogenization. An optical microscopy (OM) clearly showed the morphological development from the cellulose fibers to CNFs under repeated shear forces. The morphology, structure and properties of the obtained CNFs were comprehensively investigated using scanning electron microscopy (SEM), transmission electron microscopy (TEM), Fourier transformed infrared (FTIR) spectra, X-ray diffraction (XRD) and thermogravimetric (TG) analysis. The results indicated that the CNFs had diameters mainly ranged from 16 to 28 nm. Compared with the pulp fibers, the CNFs exhibited a slightly higher crystallinity and a lower thermal stability. Moreover, a novel nanopaper with high optical transparency was prepared from the obtained CNFs, and a possible mechanism for the high optical transparency was discussed.

1. Introduction

Cellulose is one of the most abundant natural polymers on the earth. It has a lot of extraordinary properties in terms of biocompatibility, biological degradability, and sustainability (Chen et al., 2011a; Li et al., 2012). Cellulose can be obtained from various sources, such as wood (Chen et al., 2011a), cotton (de Morais Teixeira et al., 2010), pineapple leaves (Cherian et al., 2010), sisal fibers (Madera-Santana, Soto Valdez, & Richardson, 2012), straws (Chen, Yu, Zhang, & Lu, 2011; Kaushik & Singh, 2011), sugarcane bagasse (Mandal & Chakrabarty, 2011). In nature, cellulose fibers are composed of many nanometer-sized single fibers which are bound together by hydrogen bonds. These nanofibers are usually named as nanocrystals, nanowhiskers or nanofibrils. The term "nanowhiskers" is usually used to designate elongated crystalline rod-like nanoparticles, whereas "nanofibrils" should be used to designate long flexible nanostrings consisting of alternating crystalline and amorphous regions (Eichhorn et al., 2010). The dimensions of nanocellulose are dependent on the initial source (Eichhorn, 2011). In addition to the above-mentioned advantages of cellulose, the cellulose nanofibrils (CNFs) have many other unique characteristics, such as a very large surface-to-volume ratio, high mechanical properties, and the ability to form highly porous mesh (Abraham et al., 2011). They have been extensively applied as reinforcement components in composite materials (Abraham et al., 2013b), functional fibers (Walther, Timonen, Díez, Laukkanen, & Ikkala, 2011), photoelectric materials (Nogi & Yano, 2008), as well as functional aerogels (Wu, Li, Liang, Chen, & Yu, 2013), etc. Consequently, the preparation and utilization of CNFs from renewable sources have gained much attention during the past few years.

There are several approaches to prepare nanocellulose. Concentrated acid hydrolysis is one method to extract cellulose nanowhiskers from various cellulose resources (Satyamurthy & Vigneshwaran, 2013). However, a large amount of waste acidic liquid is generated after processing. The waste leads to potential hazards to the environment. This approach is also time-consuming due to the repeated centrifuge and dialysis procedures. Furthermore, string-like nanofibrils with high aspect ratio cannot be obtained this way. Some bacteria such as *acetobacter xylinum* are able to synthesize CNFs (Klemm et al., 2009), but using bacteria can be very expensive. Recently, physical approaches such as grinding (Jonoobi, Mathew, & Oksman, 2012), cryo-crushing (Chakraborty, Sain, & Kortschot, 2005), high pressure homogenizing (Li et al., 2012; Sehaqui, Morimune, Nishino, & Berglund, 2012), became popular for extracting CNFs. A combination of two or several methods has also been tried to improve the efficiency of CNFs extraction. For instance, Fujisawa, Okita, Fukuzumi, Saito, and Isogai (2011) used TEMPO-oxidation combined with ultrasonic homogenization to make CNFs from softwood pulp. Abraham et al. (2013a) reported steam explosion followed by acid treatment could be very effective to isolate CNFs from coir fiber. Despite these successful

* Corresponding author. Tel.: +86 28 85460607; fax: +86 28 85402465.
E-mail address: weizhang@scu.edu.cn (W. Zhang).

0144-8617/$ – see front matter © 2013 Elsevier Ltd. All rights reserved.
http://dx.doi.org/10.1016/j.carbpol.2013.05.050

experiments, there are still many problems such as low efficiency, high energy consumption, high cost, which have not been solved yet.

In this study, a chemical-free refining pretreatment with high shear homogenization was used to extract CNFs. The morphology, structure and properties of the obtained nanofibrils were analyzed by optical microscope (OM), scanning electron microscope (SEM), transmission electron microscopy (TEM), Fourier transform infrared (FTIR), X-ray diffraction (XRD) and thermogravimetric analysis (TGA). The mechanism for preparing CNFs from original cellulose fibers using high shear homogenization is discussed for the first time. Furthermore, a nanopaper with high optical transparency was fabricated via simple casting.

2. Experimental

2.1. Materials

Bleached softwood pulp with cellulose content above 95%, kindly provided by the Institute of Paper Science and Technology at Georgia Tech, USA, was used as the starting materials to skip the matrix removal processes of pulping and bleaching. The pulp we used was in dry condition due to the convenience of transportation, though some researchers claimed that non-dried pulp are easier for micro-/nanofibrillation because hydrogen bonds can be regenerated between CNFs upon drying (Syverud, Chinga-Carrasco, Toledo, & Toledo, 2011). Deionized water was used throughout the experiment. No chemical reagent was involved in the experiment.

2.2. Preparation of CNFs

The dry softwood pulp board was cut into small pieces and soaked in deionized water for 24 h. A disintegrator was then used to disintegrate the softwood pulp. After the filtration of most water, the pulp was beaten for 30,000 revolutions in a PFI mill. A certain amount of deionized water was then added to dilute the pulp dispersion until a concentration of 0.5 wt%. Finally, the dispersion was processed with a high shear homogenizer (T18, IKA, Germany). The homogenization was set at a rotation speed of 22,000 rpm for 2 h. It has been found that 2 h is an optimal processing time because no further fibrillation of CNFs can be detected by SEM when the homogenization time is over 2 h, and over-homogenization (more than 2 h homogenization) will cause a decreased crystalline of CNFs and a waste of power. The homogenizing process was cooled every 5 min to prevent overheat.

2.3. Preparation of cellulose nanopaper

The cellulose nanopaper was prepared following Dufresne's method (Dufresne, Cavaillé, & Vignon, 1997). Briefly, the obtained CNFs suspension was ultrasonically treated for 10 min to evenly disperse nanofibrils. Air in the suspension was removed by pumping under vacuum in order to eliminate bubbles which can be formed in the material during drying. The dispersion was then cast into a polystyrene petri dish and stored in a fume hood at room temperature. After 48 h, the air-dried sample was stored in the desiccator for at least a week.

2.4. Characterization

2.4.1. Optical microscopy (OM)

The suspensions of treated fibers were obtained during the high shear homogenization and diluted to a concentration of 0.1 wt%. One drop of the diluted sample was dropped on a glass slide and stamped with a coverslip. An optical microscope (Leica DMLM) was used to observe the samples, and the morphology of fibers was captured by a digital imaging system.

2.4.2. Scanning electron microscopy (SEM)

The suspensions of the cellulose fibers before and after the high shear homogenization were air-dried to form sheets. The obtained thin sheets were coated with gold for 60 s using a vacuum sputter coater (Quorum Q150T ES, UK) and then observed with SEM (LEO 1530, Germany) at 10 kV. ImageJ software was used for analysis of diameter distributions of more than 100 cellulose fibers or CNFs selected randomly from the SEM images.

2.4.3. Transmission electron microscopy (TEM)

A drop of diluted aqueous CNFs suspension was deposited on the carbon-coated grids, which was then dried under table lamp. After the specimen has been completely dried, it was observed using TEM (Tecnai G^2 F20, Holland) with an acceleration voltage of 80 kV.

2.4.4. Fourier transform infrared spectroscopy (FTIR)

The FTIR spectra of CNFs and raw cellulose fibers were recorded on a Fourier transform infrared spectrometer (Nicolet Magna-IR 550, USA). The samples were dried at 80 °C under vacuum for 12 h before analysis. Then a small quantity (2 mg) of sample was blended with KBr powder (300 mg) and compressed to form a disk. The spectra for each sample were recorded as an average of 100 scans in the range from 4000 to 400 cm^{-1} at a resolution of 2 cm^{-1}.

2.4.5. X-ray diffraction (XRD)

The crystallinity of softwood cellulose fibers and CNFs was examined by high resolution X-ray diffractometer (Philips Analytical X'Pert, Netherlands) with nickel filtered Cu Kα radiation ($\lambda = 0.1540$ nm) at 40 kV and 40 mA. Scattered radiation was detected in the range $2\theta = 5–30°$ with a step interval of 0.02°. The crystallinity index (CrI) was calculated by Segal's method (Segal, Creely, Martin, & Conra, 1959) using the equation given by

$$\mathrm{CrI} = \frac{(I_{002} - I_{\mathrm{am}})}{I_{002}} \times 100 \quad (1)$$

where I_{200} is the intensity value for the crystalline cellulose close to 22°, and I_{am} is the intensity value for the amorphous cellulose close to 18°.

2.4.6. Thermal analysis

Thermogravimetric analysis (TGA) and derivative thermogravimetric analysis (DTG) were carried out with a synchronous thermal analysis system (STA 6000, Perkin Elmer, USA). Approximately 10 mg of sample was used for each testing. Temperature programs for dynamic tests were from 30 °C to 500 °C at four different heating rates (5, 20 and 30 °C/min) under an air flow of 40 mL/min.

3. Results and discussion

3.1. Morphology observation by OM

OM analysis was carried out to observe the morphological development of softwood nanofibers during high shear homogenization at micron level. Fig. 1(a) shows that the diameters of pristine softwood cellulose fibers are between 20 and 50 μm. It has been well known that the refining process prior to homogenization is a key step to reduce energy consumption for the isolation of CNFs, because it helps to soften and to loosen the structure of cellulose fibers. This process not only produces external fibrillation by raising fine fibers on the surface layers (P and S1 layers) via abrasive action, but also makes internal fibrillation by breaking links between CNFs (Stelte & Sanadi, 2009). From Fig. 1(b), it is evident that the refining treatment by PFI mill made the fibers much looser, and generated

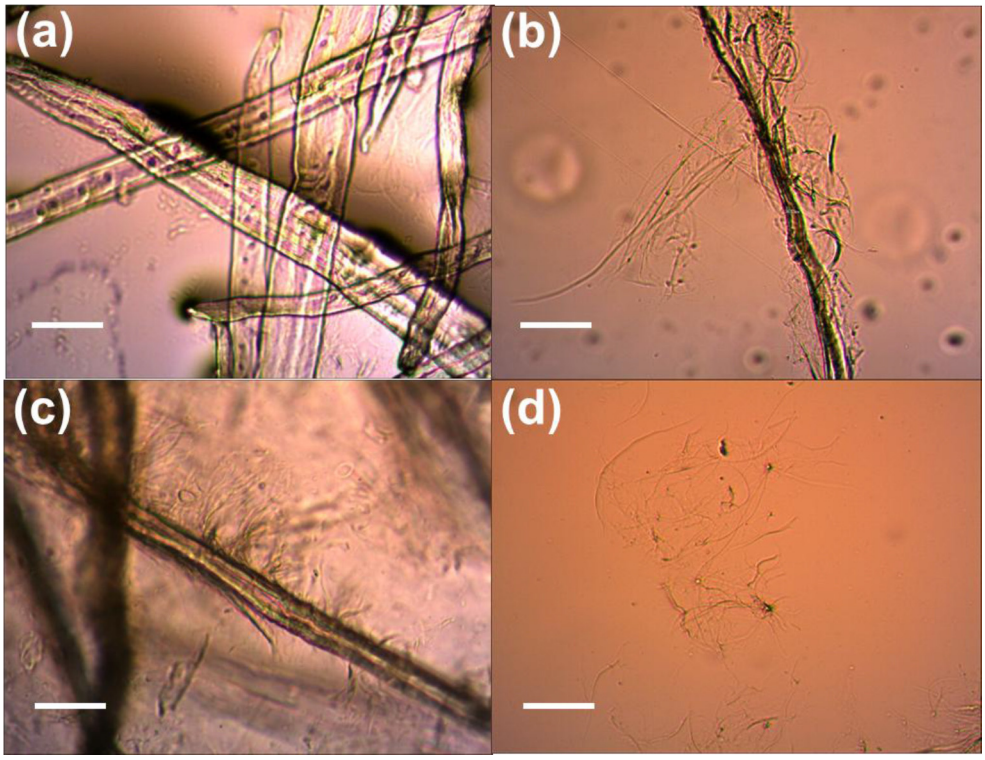

Fig. 1. The morphological development of softwood cellulose fibers during high shear homogenization processing visualized from optical microscope. (a) Pristine softwood cellulose fibers. (b) Softwood fibers after PFI mill refining. (c) Softwood fibers after 10 min high shear homogenization. (d) Softwood fibers after refining and 60 min high shear homogenization. The scale bar is 50 μm.

many thin fibrils on the fiber surface. Thereafter, the refined fibers were subjected to a high shear homogenizer. To better understand the effect of mechanical shear force on the fibrillation of cellulose fibers, raw fibers suspension without refining were directly homogenized. As shown in Fig. 1(c), 10 min high shear homogenization created lots of tiny fibrils on the fiber surface by gradually peeling off them from the outer layer. Fig. 1(d) exhibits the representative morphology of the obtained CNFs after combined treatments of refining and 60 min high shear homogenization. Cellulose fibrils with very thin diameters were obtained.

3.2. Morphology observation by SEM and TEM

OM is a simple and convenient tool to observe materials in the micrometer scale. However, it is not possible to give detailed morphological information of materials in the nanoscale due to the limitation of the equipment which uses visible light. SEM was conducted for observing the obtained CNFs in the nanoscale. Fig. 2(a) and (c) represents SEM images of pristine softwood pulp fibers and as-prepared CNFs, respectively. Fig. 2(b) and (d) are diagrams of fiber diameters distribution counted from the SEM images using the software of Image J. The SEM images clearly reveal that the cellulose fibers were almost completely disintegrated into CNFs after high shear homogenization although several CNFs bundles with relatively larger size still exist. The diameters of pristine softwood cellulose fibers were mainly distributed in the range of 20–45 μm. However, the diameters of most of the CNFs were between 16 and 28 nm, 4 orders of magnitude smaller than those of raw materials. The nano dimension of obtained CNFs was also well supported by TEM analysis. The inserted TEM image in Fig. 2(c) demonstrates that the diameters of most of CNFs are thinner than 30 nm. This value is similar to the reports on other nanofibrillation methods (Abe, Iwamoto, & Yano, 2007; Chen et al., 2011a), indicating the feasibility and high effectiveness of our approach using the high shear homogenization.

The possible mechanism for the nanofibrillation of cellulose fibers is demonstrated in Fig. 3. The main component of the high shear homogenizer is the homogeneous head with a stator–rotor structure. The impeller-like rotor is usually called stirring impeller. When the rotor is rotating at a high speed driven by the motor, cellulose fibers can be sucked into the cavity formed by the rotor and the stator. The cellulose fibers are strongly suffered from hydraulic shear, fluid layer friction, centrifugal extrusion and collision tearing in the cavity. Consequently, CNFs can be gradually peeled off from the cellulose fibers, and also the hydrogen bonds between nanofibrils can be partially broken. After numerous repeating cycles, stable and well dispersed CNFs dispersions could be obtained.

3.3. FTIR analysis

The influence of high shear homogenization on the molecular and supramolecular structures of cellulose was studied by FTIR. Fig. 4 illustrates the transmittance FTIR spectra of the pristine softwood cellulose fibers and the CNFs prepared by high shear homogenization. The dominant peaks of pristine softwood cellulose are in consistent with those of pure cellulose (Pandey, 1999). It suggested that the softwood pulp was most made of cellulose, with very few hemicellulose, lignin or other substances after pulping and bleaching. There was no new absorption peak that appears for CNFs. This absence of peak indicated that no new functional groups were generated during the mechanical homogenization process. However, the absorption intensity of the peaks changed a bit, revealing that the molecular and supramolecular structures were affected by the high shear homogenization. The characteristic peak of O—H stretching in the region from 3700 cm^{-1} to 2950 cm^{-1} became narrower after treatment. This phenomenon indicates the hydrogen bonds in cellulose, presumably the hydrogen bonds between CNFs

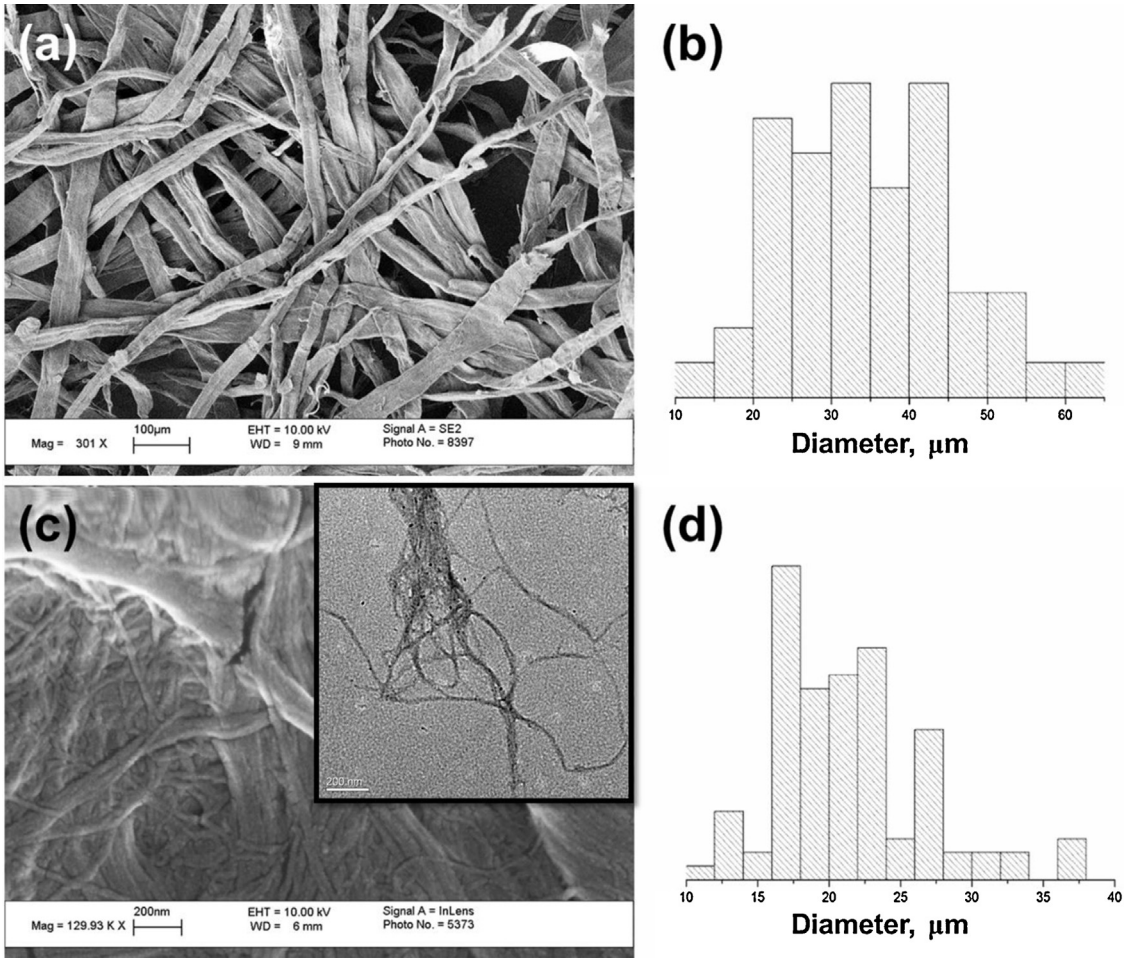

Fig. 2. FE-SEM micrographs of the (a) pristine softwood cellulose fibers (the scale bar is 100 μm), (c) softwood cellulose fibers after refining and 60 min high shear homogenization (the scale bar is 200 nm), the inserted TEM image in (c) reveals the morphology of some individual CNFs (the scale bar is 200 nm); and diameter distribution of (b) pristine softwood cellulose fiber, (d) softwood cellulose fibers after refining and 60 min high shear homogenization.

within cellulose fibers, were destroyed due to the strong shear forces exerted by the homogenizer. In addition, the intensity of O—H stretching absorption peak was increased after homogenization, suggesting that more free hydroxyl groups were exposed in cellulose (Abraham et al., 2013a).

3.4. X-ray diffraction analysis

XRD analysis of pristine cellulose fibers and CNFs were conducted in order to study the effect of homogenization on the crystalline structure of cellulose. Fig. 5 shows the de-convolution spectra of XRD aided by the software of Jade 5. It is clear that both diffractograms exhibits a sharp peak around $2\theta = 22.7^{\circ}$ corresponding to (0 0 2) lattice plane and two overlapped weaker diffractions at $2\theta = 14.8^{\circ}$ and $2\theta = 16.3^{\circ}$ assigned to (1 0 1) and ($1\,0\,1^{-}$) lattice plane of cellulose I (Besbes, Vilar, & Boufi, 2011). The XRD data indicates that the crystal type of cellulose was not influenced upon high shear homogenization. However, both the crystallinity (estimated by Jade 5) and crystallinity index (CI) of CNFs were consistently increased as compared with pristine fibers. The crystallinity and CI were increased from 73.2% and 77.2% to 78.1% and 79.5%, respectively, indicating the shear forces exerted by homogenizer are mainly focused on the weak amorphous region of cellulose fibers, making the resulting CNFs a higher crystallinity. Tonoli et al. found that the CI of CNFs isolated by sonication was sharply decreased from 69% of raw fibers to 33% (Tonoli et al., 2012). In this sense, the high shear homogenization has obvious advantages over sonication to produce CNFs with less negative influences on their crystallinity. The CNFs extracted by high shear homogenization are more suitable as the reinforcing element in composites making. This is because highly crystalline CNFs can be more effective to achieve higher reinforcement for composite materials (Chen et al., 2011a).

3.5. TG/DTG analysis

TGA at different heating rates was run under an air flow to study the thermal oxidative degradation of cellulose samples. As far as we know, most of TGA studies of CNFs are performed under inert gas (Abraham et al., 2011; Li et al., 2012). However, the practical processing and application of CNFs are usually performed in air. Therefore, the presented data here may be more reliable in such conditions.

The TG and DTG curves for pristine cellulose fibers and CNFs were illustrated in Fig. 6. Consistent with previous reports, the mass loss on the TG curves for both samples can be divided into three zones (Cabrales & Abidi, 2010; Ramiah, 1970). The first zone starts at 30–50 °C and finishes at 150–180 °C. This zone represents a slight mass loss (about 5%) for the evaporation of water that exists in the cellulose fibers. This phase corresponds to the small peak on the left side of DTG curves. A sharp weight loss representing the main pyrolysis step of cellulose in the second zone (from 250–300 °C to 300–350 °C) then happens. This loss corresponds to a dominant peak on the DTG curves. During this stage, the molecular chains of the cellulose fracture, and they gradually transform

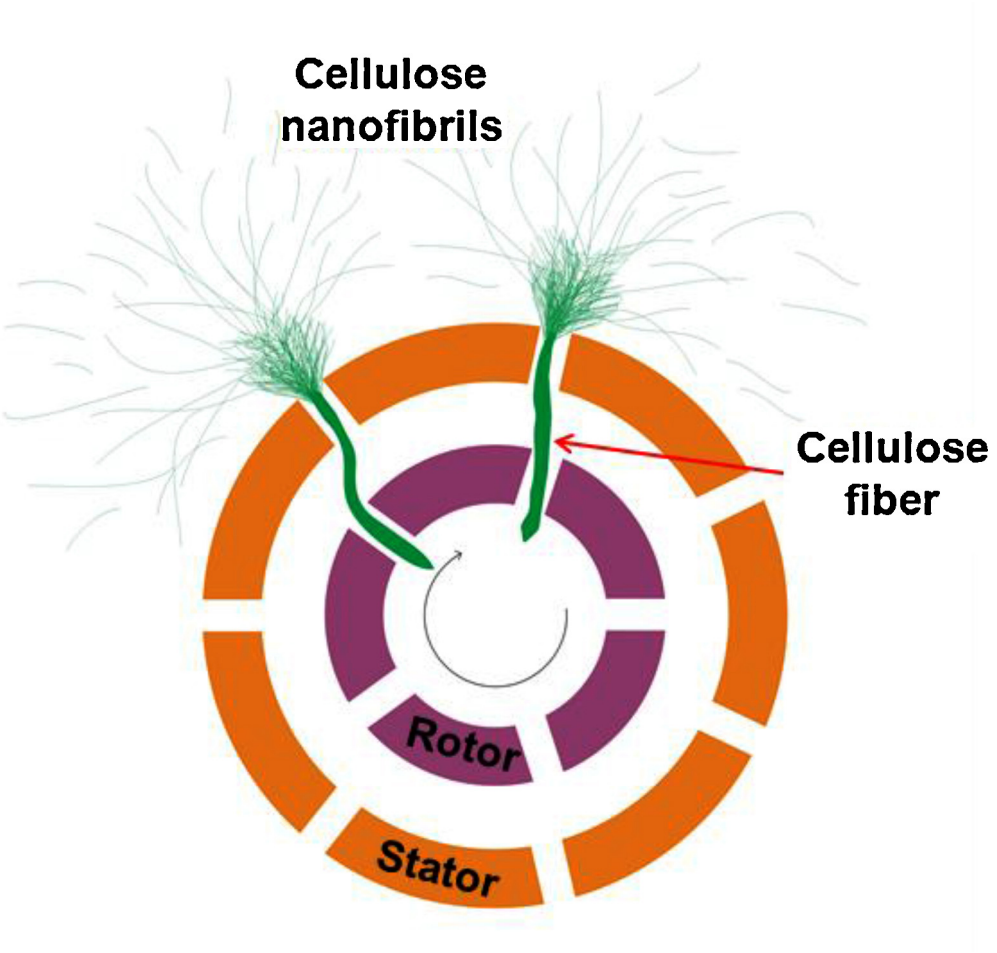

Fig. 3. Schematic diagram of the fibrillation process of cellulose fiber under high shear homogenization.

into CO_2 and volatile hydrocarbons. The mass of the cellulose fibers decreases rapidly by about 70%. The third zone (from 300–360 °C to 410–510 °C) can be seen as a tail in TG curves where the weight loss of cellulose slows down. This zone is identified as the thermal oxidative decomposition of the char. According to literatures, a considerable amount of char will remain after TGA tests of cellulose under an inert atmosphere (Chen et al., 2011b; Li et al., 2012). However, in this study, the cellulose samples were almost completely burned out because of the continuing thermal oxidative degradation of the char produced during the second stage.

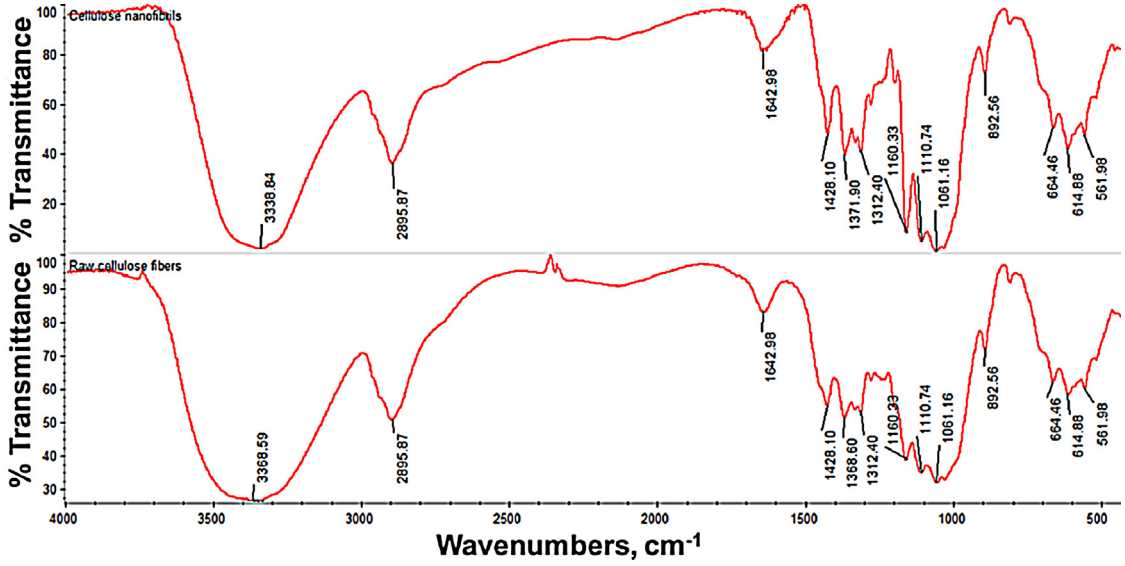

Fig. 4. Fourier transform infrared spectroscopy of pristine softwood cellulose fibers and softwood CNFs produced by high shear homogenization.

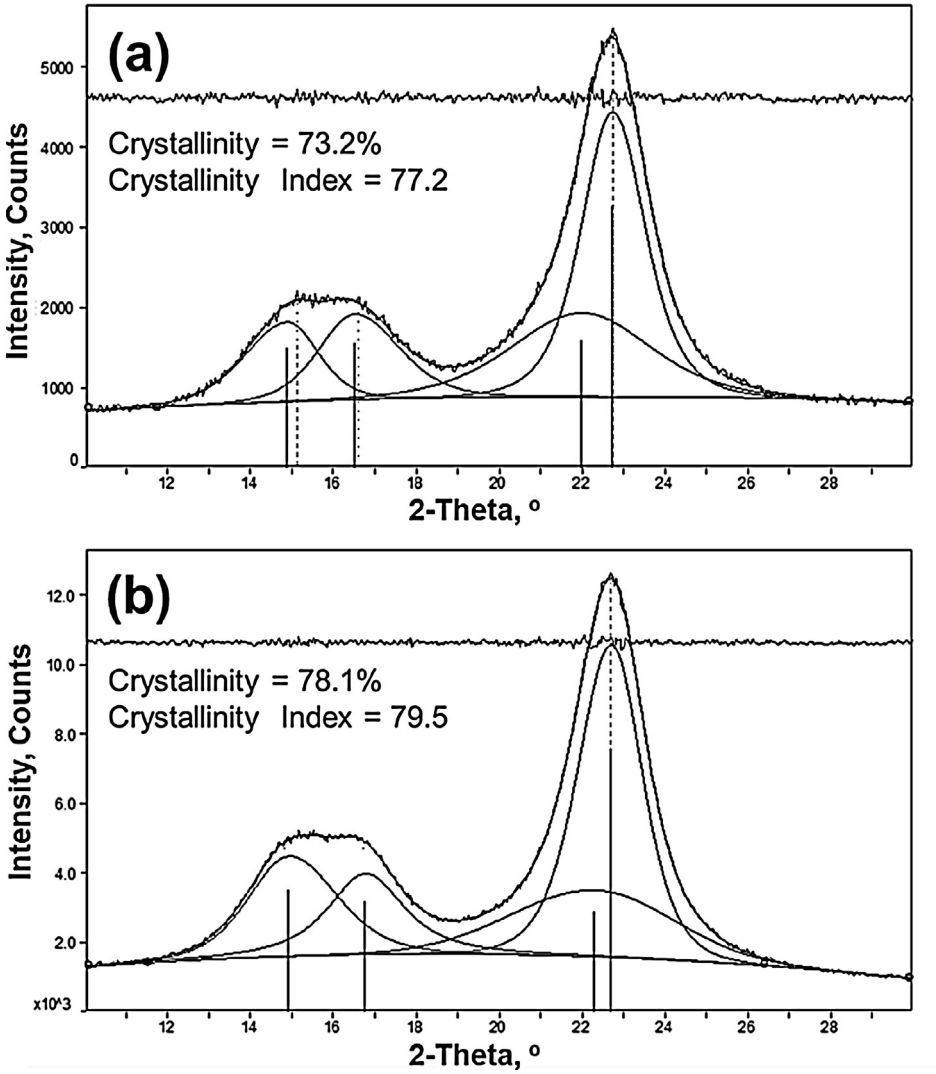

Fig. 5. The XRD deconvolution spectra of (a) pristine softwood cellulose fibers, and (b) softwood CNFs after refining and 60 min high shear homogenization.

The thermal degradation parameters of CNFs and pristine softwood cellulose fibers from TG and DTG analysis are shown in Table 1. The initial decomposing temperature (T_i) and the temperature at maximum decomposing (T_{max}) of CNFs are lower than those of pristine fibers, suggesting an inferior thermal stability of the CNFs. A possible reason is that CNFs have more contact points compare with raw cellulose fibers. Therefore, when one nanofibril starts to degrade, it can induce the thermal degradation of the surrounding nanofibrils (Quiévy et al., 2010). Some researchers (Abraham et al., 2011) reported a higher thermal stability for the extracted CNFs compared with the starting fibers. A main reason for the difference is that Abraham et al. used raw plant fibers as starting materials which contained a considerable amount of matrix substances with lower thermal stability, such as hemicellulose, ligin, etc. Table 1 also shows that T_i and T_{max} increase with increasing heating rate. This phenomenon is explained by the fact that heat transfer is time-dependent which results in delayed decomposition when heating at a higher rate.

3.6. Optical transparency of cellulose nanopaper

The nanopaper was fabricated by casting the CNFs suspension. The nanopaper is highly transparent as shown in Fig. 7(a). The Sichuan University logo can be seen underneath a piece of nanopaper that has a thickness of 60 μm. In contrast, the ordinary paper (Fig. 7(b)) is non-transparent. Although both papers are comprised

Table 1
Thermal degradation parameters of cellulose from TGA and DTG analysis.

Heating rate	Raw fibers		CNFs	
	T_i (°C)	T_{max} (°C)	T_i (°C)	T_{max} (°C)
5 °C/min	280.86 ± 0.36	325.23 ± 0.79	246.27 ± 0.09	299.76 ± 0.55
20 °C/min	311.33 ± 1.07	349.72 ± 0.88	262.24 ± 0.91	308.03 ± 1.19
30 °C/min	318.48 ± 0.65	357.34 ± 1.08	266.45 ± 0.95	315.16 ± 0.63

Note: T_i is the initial decomposing temperature, and T_{max} is the temperature at the maximum decomposing rate.

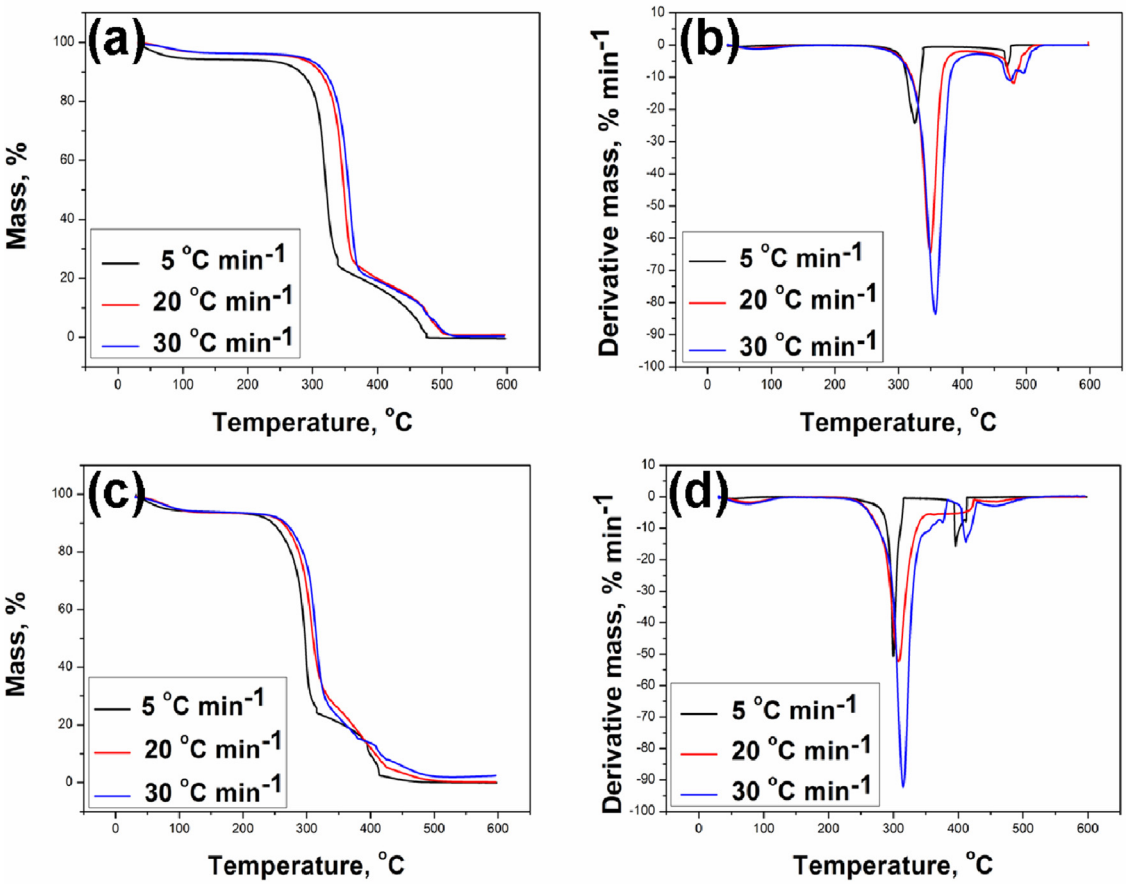

Fig. 6. TG curves of pristine softwood cellulose fibers (a) and CNFs (c), and DTG curve of pristine softwood cellulose fibers (b) and CNFs (d) at different heating rates.

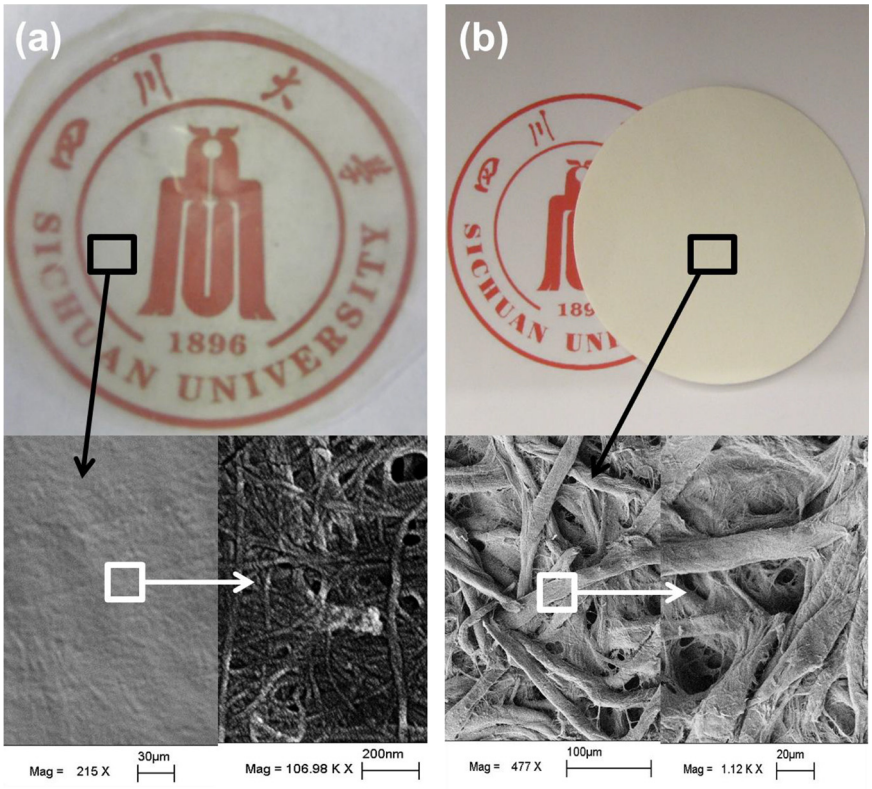

Fig. 7. Light transmittance of nanopaper (a) and ordinary paper (b), and their microstructure from SEM imaging.

of the same substance, their optical properties are totally different. It is well known that visible light is a kind of electromagnetic wave. Theoretically, visible light can pass through fibers of diameters less than 400 nm without refraction and reflection at air/fiber interface (Tang & Liu, 2008). However, when the diameter of fibers is larger than 400 nm, light refraction and reflection will happen. As a result, the transmitted light decreases remarkably. From Fig. 7, it is evident that the nanopaper is built up by CNFs with diameters of about 20 nm. During the formation of nanopaper, CNFs were compacted tightly owing to the high surface tension of water when evaporated. As a result, large pores, which could reduce the optical transparency, were also eliminated. On the other hand, the diameters of cellulose fibers inside ordinary paper are much larger than 400 nm (about 20–50 μm). Because the refractive indexes of air and cellulose are different, refraction and reflection will occur at the interface of cellulose and air, leading to a reduced light transmittance. In addition, there are a lot of large holes among cellulose fibers, which causes serious light scattering. Therefore, the ordinary paper is optically opaque.

4. Conclusions

In this study, CNFs were successfully extracted from dry softwood pulp board by combined methods of mechanical refining pretreatment with high shear homogenization. The OM showed that CNFs were peeled off from the cellulose fibers by the shear force. SEM and TEM analysis confirmed that the diameter of CNFs were mainly in the range of 16–28 nm. FTIR measurements of the fibers revealed that hydrogen bonds were partially destroyed during the homogenization process. The CNFs had a higher crystallinity compared with the pulp fibers, possibly because the destruction caused by shear force was more favored at the amorphous region of cellulose. TG and DTG analysis indicated that the thermal stability of CNFs decreased as compared to cellulose fibers. Optically transparent nanopaper was fabricated from CNFs suspension by casting, which could be potentially used as optical components for advanced applications. To sum up, we demonstrated that high shear homogenization could be an effective method to extract high quality CNFs from lignocellulose fibers.

Acknowledgements

The authors would like to thank Natural Science Foundation of China (50833003 and 51203105) and Young Scholar Fund of Sichuan University (2012SCU11074) for financial support of this work. Miss Soyire M. Coulibaly from School of Chemical and Biomolecular Engineering at Georgia Tech is gratefully acknowledged for her contributions to the English improvement of this paper.

References

Abe, K., Iwamoto, S., & Yano, H. (2007). Obtaining cellulose nanofibers with a uniform width of 15 nm from wood. *Biomacromolecules*, *8*, 3276–3278.

Abraham, E., Deepa, B., Pothan, L. A., Jacob, M., Thomas, S., Cvelbar, U., et al. (2011). Extraction of nanocellulose fibrils from lignocellulosic fibres: A novel approach. *Carbohydrate Polymers*, *86*, 1468–1475.

Abraham, E., Deepa, B., Pothen, L. A., Cintil, J., Thomas, S., John, M. J., et al. (2013). Environmental friendly method for the extraction of coir fibre and isolation of nanofiber. *Carbohydrate Polymers*, *92*, 1477–1483.

Abraham, E., Deepa, B., Pothan, L. A., John, M., Narine, S. S., Thomas, S., et al. (2013). Physicomechanical properties of nanocomposites based on cellulose nanofibre and natural rubber latex. *Cellulose*, *20*, 417–427.

Besbes, I., Vilar, M. R., & Boufi, S. (2011). Nanofibrillated cellulose from TEMPO-oxidized eucalyptus fibres: Effect of the carboxyl content. *Carbohydrate Polymers*, *84*, 975–983.

Cabrales, L., & Abidi, N. (2010). On the thermal degradation of cellulose in cotton fibers. *Journal of Thermal Analysis and Calorimetry*, *102*, 485–491.

Chakraborty, A., Sain, M., & Kortschot, M. (2005). Cellulose microfibrils: A novel method of preparation using high shear refining and cryocrushing. *Holzforschung*, *59*, 102–107.

Chen, W., Yu, H., Liu, Y., Chen, P., Zhang, M., & Hai, Y. (2011). Individualization of cellulose nanofibers from wood using high-intensity ultrasonication combined with chemical pretreatments. *Carbohydrate Polymers*, *83*, 1804–1811.

Chen, X., Yu, J., Zhang, Z., & Lu, C. (2011). Study on structure and thermal stability properties of cellulose fibers from rice straw. *Carbohydrate Polymers*, *85*, 245–250.

Cherian, B. M., Leão, A. L., Souza, S. F., Thomas, S., Pothan, L. A., & Kottaisamy, M. (2010). Isolation of nanocellulose from pineapple leaf fibres by steam explosion. *Carbohydrate Polymers*, *81*, 720–725.

de Morais Teixeira, E., Corrêa, A., Manzoli, A., de Lima Leite, F., de Oliveira, C., & Mattoso, L. (2010). Cellulose nanofibers from white and naturally colored cotton fibers. *Cellulose*, *17*(3), 595–606.

Dufresne, A., Cavaillé, J., & Vignon, M. R. (1997). Mechanical behavior of sheets prepared from sugar beet cellulose microfibrils. *Journal of Applied Polymer Science*, *64*, 1185–1194.

Eichhorn, S. J. (2011). Cellulose nanowhiskers: Promising materials for advanced applications. *Soft Matter*, *7*, 303–315.

Eichhorn, S. J., Dufresne, A., Aranguren, M., Marcovich, N. E., Capadona, J. R., Rowan, S. J., et al. (2010). Review: Current international research into cellulose nanofibres and nanocomposites. *Journal of Materials Science*, *45*, 1–33.

Fujisawa, S., Okita, Y., Fukuzumi, H., Saito, T., & Isogai, A. (2011). Preparation and characterization of TEMPO-oxidized cellulose nanofibril films with free carboxyl groups. *Carbohydrate Polymers*, *84*, 579–583.

Jonoobi, M., Mathew, A. P., & Oksman, K. (2012). Producing low-cost cellulose nanofiber from sludge as new source of raw materials. *Industrial Crops and Products*, *40*, 232–238.

Kaushik, A., & Singh, M. (2011). Isolation and characterization of cellulose nanofibrils from wheat straw using steam explosion coupled with high shear homogenization. *Carbohydrate Research*, *346*, 76–85.

Klemm, D., Schumann, D., Kramer, F., Heßler, N., Koth, D., & Sultanova, B. (2009). Nanocellulose materials – Different cellulose, different functionality. *Macromolecular Symposia*, *280*, 60–71.

Li, J., Wei, X., Wang, Q., Chen, J., Chang, G., Kong, L., et al. (2012). Homogeneous isolation of nanocellulose from sugarcane bagasse by high pressure homogenization. *Carbohydrate Polymers*, *90*, 1609–1613.

Madera-Santana, T. J., Soto Valdez, H., & Richardson, M. O. W. (2012). Influence of surface treatments on the physicochemical properties of short sisal fibers: Ethylene vinyl acetate composites. *Polymer Engineering & Science*, *53*, 59–68.

Mandal, A., & Chakrabarty, D. (2011). Isolation of nanocellulose from waste sugarcane bagasse (SCB) and its characterization. *Carbohydrate Polymers*, *86*, 1291–1299.

Nogi, M., & Yano, H. (2008). Transparent nanocomposites based on cellulose produced by bacteria offer potential innovation in the electronics device industry. *Advanced Materials*, *20*, 1849–1852.

Pandey, K. K. (1999). A study of chemical structure of soft and hardwood and wood polymers by FTIR spectroscopy. *Journal of Applied Polymer Science*, *71*, 1969–1975.

Quiévy, N., Jacquet, N., Sclavons, M., Deroanne, C., Paquot, M., & Devaux, J. (2010). Influence of homogenization and drying on the thermal stability of microfibrillated cellulose. *Polymer Degradation and Stability*, *95*, 306–314.

Ramiah, M. V. (1970). Thermogravimetric and differential thermal analysis of cellulose, hemicellulose, and lignin. *Journal of Applied Polymer Science*, *14*, 1323–1337.

Satyamurthy, P., & Vigneshwaran, N. (2013). A novel process for synthesis of spherical nanocellulose by controlled hydrolysis of microcrystalline cellulose using anaerobic microbial consortium. *Enzyme and Microbial Technology*, *52*, 20–25.

Segal, L., Creely, J. J., Martin, A. E., Jr., & Conra, C. M. (1959). An empirical method for estimating the degree of crystallinity of native cellulose using the X-ray diffractometer. *Textile Research Journal*, *29*, 786–794.

Sehaqui, H., Morimune, S., Nishino, T., & Berglund, L. A. (2012). Stretchable and strong cellulose nanopaper structures based on polymer-coated nanofiber networks: An alternative to nonwoven porous membranes from electrospinning. *Biomacromolecules*, *13*, 3661–3667.

Stelte, W., & Sanadi, A. R. (2009). Preparation and characterization of cellulose nanofibers from two commercial hardwood and softwood pulps. *Industrial & Engineering Chemistry*, *48*, 11211–11219.

Syverud, K., Chinga-Carrasco, G., Toledo, J., & Toledo, P. G. (2011). A comparative study of Eucalyptus and Pinus radiatapulp fibres as raw materials for production of cellulose nanofibrils. *Carbohydrate Polymers*, *84*, 1033–1038.

Tang, C., & Liu, H. (2008). Cellulose nanofiber reinforced poly(vinyl alcohol) composite film with high visible light transmittance. *Composites Part A: Applied Science and Manufacturing*, *39*, 1638–1643.

Tonoli, G. H. D., Teixeira, E. M., Corrêa, A. C., Marconcini, J. M., Caixeta, L. A., Pereira-da-Silva, M. A., et al. (2012). Cellulose micro/nanofibres from Eucalyptus kraft pulp: Preparation and properties. *Carbohydrate Polymers*, *89*, 80–88.

Walther, A., Timonen, J. V. I., Díez, I., Laukkanen, A., & Ikkala, O. (2011). Multifunctional high-performance biofi bers based on wet-extrusion of renewable native cellulose nanofibrils. *Advanced Materials*, *23*, 2924–2928.

Wu, Z., Li, C., Liang, H., Chen, J., & Yu, S. (2013). Ultralight, flexible, and fire-resistant carbon nanofiber aerogels from bacterial cellulose. *Angewandte Chemie*, *125*, 2997–3001.